JMEPEG (1998) 7:637-642 ©ASM International

Heat Transfer Coefficient on External Mold Surface at High Pressure and Application to Metal-Matrix Composite Casting

J. Yang and O.J. Ilegbusi

(Submitted 29 December 1997; in revised form 28 May 1998)

A relationship is established between the heat transfer coefficient on the external surface of a mold and the ambient temperature and pressure within the operating range typical of pressure-infiltration casting of metal-matrix composites. This relationship is based on existing data and correlation for the thermophysical properties of the ambient nitrogen. The predicted temperature profiles are in good agreement with the experimental data obtained for a metal-matrix composite casting process. The application of the established relationship is carried beyond the experimental evidence to predict the solidification pattern in the pressure-casting system.

Keywords heat transfer coefficient, high pressure, metal-matrix composite, mold surface

1. Introduction

Many industrial processes are operated in a high pressure environment in which convective heat transfer from a hot surface significantly influences the properties of the final product. In some cases, as in the pressure infiltration of metal-matrix composites, the external surfaces of the mold are exposed to pressurized gas, the thermophysical properties of which vary widely over the pressure range of interest. Correspondingly, the heat transfer coefficient on these surfaces may change significantly enough to affect the solidification pattern in the mold. Yet, there exists no systematic and fundamental study of how this heat transfer coefficient can be reliably determined, at least within the context of pressure-infiltrated composite casting. The objective of this study is to develop a simple formulation relating the heat transfer coefficient to the properties of the ambient nitrogen, pressure, and temperature, which will be applicable to high-pressure casting systems.

Several theoretical and experimental studies have been done on heat transfer by free convection from vertical surfaces. In the laminar regime, the works of Ede (Ref 1) and Churchill and Usagi (Ref 2) are worth noting. For turbulent situations, some empirical expressions have been developed by Churchill and Chu (Ref 3), Bosworth (Ref 4), Saunders (Ref 5), and Bayley (Ref 6). Although these expressions have been successfully applied to processing under normal atmospheric pressure, their extension to high-pressure conditions has not been systematically investigated.

In this paper, a simple relation is developed for the space-mean value of the heat transfer coefficient on a mold surface exposed to high-pressure nitrogen environment. This relation is then used to model the thermal history and solidification phenomena in a pressure-infiltrated metal-matrix composite casting process. The predicted results are compared with the temperature profiles measured at several locations during the casting operation. In addition, the effect of this coefficient on the solidification pattern in the mold is investigated.

J. Yang and **O.J. Ilegbusi,** Department of Mechanical, Industrial and Manufacturing Engineering, Northeastern University, Boston, MA 02115, USA.

2. Problem Considered

Consider a mold containing hot metal, metal alloy, or composite placed in a chamber pressurized with gaseous nitrogen, as shown in Fig. 1. The mold surface may or may not be insulated from the ambient gas. The objective is to determine the effective heat transfer coefficient at the outer mold surface that is exposed to the ambient nitrogen. A practical embodiment of such a problem is the pressure-infiltrated metal-matrix composite casting process shown in Fig. 2. The system consists of an alumina preform fully infiltrated with Al 2014 alloy in a graphite mold. The infiltration and casting are carried out in a pressure chamber. The vertical surfaces of the mold are partially insulated while heat is removed through a chill at the bottom surface. The heat transfer correlation established based on the generic situation in Fig. 1 is used to prescribe the thermal

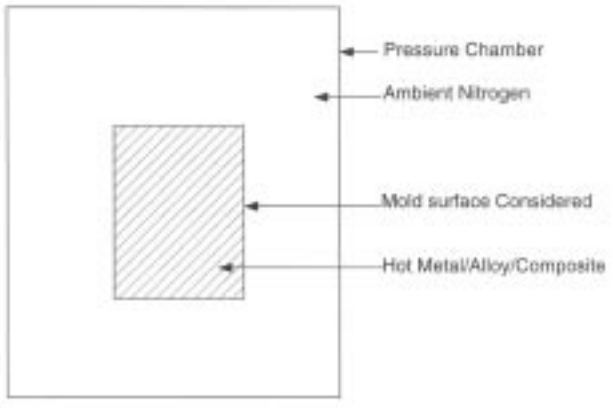

Fig. 1 Schematic of generic problem considered

boundary condition for the real system in Fig. 2. The predictions include comparison of the temperature profiles with the experimental data and the solidification pattern inside the mold.

3. Properties of Ambient Nitrogen at High Pressure

The heat transfer coefficient on the outer mold surface depends on the thermophysical properties of the ambient nitrogen under high pressure. These properties include the density ρ, specific heat C_p, viscosity μ, thermal conductivity *k*, and coefficient of thermal expansion β. The effect of pressure on these properties has been extensively studied, and valuable relations and data have been established (Ref 7-10). The relations used to determine the heat transfer coefficient are presented below.

3.1 Density

The density of nitrogen can be obtained through the following state equation (Ref 7):

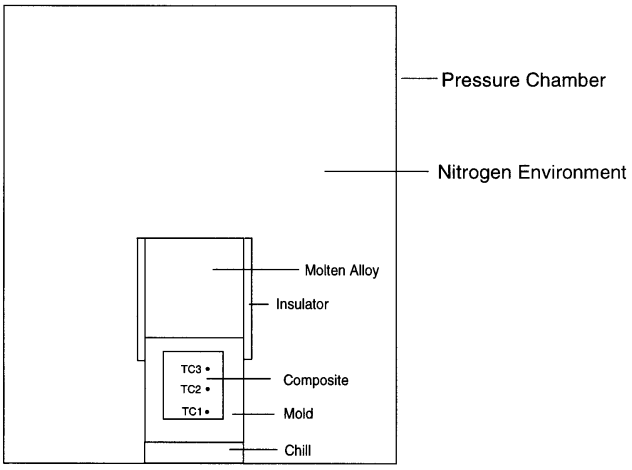

Fig. 2 Schematic of MMC system considered showing thermocouple locations TC1, TC2, TC3

$$P = \rho RT + \rho^2\left(A_1T + A_2T^{1/2} + A_3 + \frac{A_4}{T} + \frac{A_5}{T^2}\right) + \rho^3\left(A_6T + A_7 + \frac{A_8}{T} + \frac{A_9}{T^2}\right) + \rho^4\left(A_{10}T + A_{11} + \frac{A_{12}}{T}\right) + \rho^5(A_{13}) + \rho^6\left(\frac{A_{14}}{T} + \frac{A_{15}}{T^2}\right) + \rho^7\left(\frac{A_{16}}{T}\right) + \rho^8\left(\frac{A_{17}}{T} + \frac{A_{18}}{T^2}\right) + \rho^9\left(\frac{A_{19}}{T^2}\right) + \rho^3\left(\frac{A_{so}}{T^2} + \frac{A_{21}}{T^3}\right)\exp(-\gamma\rho^2) + \rho^5\left(\frac{A_{22}}{T^2} + \frac{A_{23}}{T^4}\right)\exp(-\gamma\rho^2) + \rho^7\left(\frac{A_{24}}{T^2} + \frac{A_{25}}{T^3}\right)\exp(-\gamma\rho^2) + \rho^9\left(\frac{A_{26}}{T^2} + \frac{A_{27}}{T^4}\right)\exp(-\gamma\rho^2) + \rho^{11}\left(\frac{A_{28}}{T^2} + \frac{A_{29}}{T^3}\right)\exp(-\gamma\rho^2) + \rho^{13}\left(\frac{A_{30}}{T^2} + \frac{A_{31}}{T^3} + \frac{A_{32}}{T^4}\right)\exp(-\gamma\rho^2) \quad \text{(Eq 1)}$$

where *P* is the pressure , ρ is the density, *T* is the temperature, and γ and the coefficients A_1 to A_{32} are empirical constants. Jacobsen (Ref 7) obtained this state equation by performing a stepwise multiple regression analysis on a variety of data for nitrogen, and the coefficients were determined by a weighted least squares fit to the selected data. In effect, the additional terms on the right hand side express the deviation from the ideal gas relation.

3.2 Heat Capacity

The heat capacity, C_p, for the ambient nitrogen can be expressed (Ref 8):

$$C_p = R\left(\frac{B_1}{T^3} + \frac{B_2}{T^2} + \frac{B_3}{T} + B_4 + B_5T + B_6T^2 + B_7T^3 + B_8\frac{(B_9/T)^2\, e^{\,B_9/T}}{(e^{\,B_9/T} - 1)^2}\right) \quad \text{(Eq 2)}$$

Table 1 Constants used in the study

$A_1 = 0.136224769272827 \times 10^{-2}$
$A_2 = 0.107032469908591$
$A_3 = -0.243900721871413 \times 10^{1}$
$A_4 = 0.341007449376470 \times 10^{2}$
$A_5 = -0.422374809466167 \times 10^{4}$
$A_6 = 0.105098699246494 \times 10^{-3}$
$A_7 = -0.112594826522081 \times 10^{-1}$
$A_8 = 0.142699789270907 \times 10^{-3}$
$A_9 = 0.184698501609007 \times 10^{5}$
$A_{10} = 0.811140082588776 \times 10^{-7}$
$A_{11} = 0.233011645038006 \times 10^{-2}$
$A_{12} = -0.507752586350986$
$A_{13} = 0.485027881931214 \times 10^{-4}$
$A_{14} = -0.113656764115364 \times 10^{-2}$
$A_{15} = -0.707430273540575$
$A_{16} = 0.751706648852680 \times 10^{-4}$
$A_{17} = -0.111614119537424 \times 10^{-5}$
$A_{18} = 0.368796562233495 \times 10^{-3}$
$A_{19} = -0.201317691347729 \times 10^{-5}$
$A_{20} = -0.169717444755949 \times 10^{5}$
$A_{21} = -0.119719240044192 \times 10^{6}$
$A_{22} = -0.975218272038281 \times 10^{2}$
$A_{23} = 0.554639713151823 \times 10^{5}$
$A_{24} = -0.179920450443470$
$A_{25} = -0.256242926077184 \times 10^{1}$
$A_{26} = -0.413707715090789 \times 10^{-3}$
$A_{27} = -0.256245415300293$
$A_{28} = -0.124222373740063 \times 10^{-6}$
$A_{29} = 0.103556535840165 \times 10^{-4}$
$A_{30} = -0.538699166558303 \times 10^{-9}$
$A_{31} = -0.757415412839596 \times 10^{-8}$
$A_{32} = 0.585367172069521 \times 10^{-7}$
$\gamma = 0.0056$
$B_1 = -0.735210401157252 \times 10^{3}$
$B_2 = 0.342239980411978 \times 10^{2}$
$B_3 = -0.557648284567620$
$B_4 = 0.350404228308756 \times 10^{1}$
$B_5 = -0.173390185081005 \times 10^{4}$
$B_6 = 0.174659849766463 \times 10^{-7}$
$B_7 = -0.356892033544348 \times 10^{-11}$
$B_8 = 0.199538722808834 \times 10^{1}$
$B_9 = 0.335340610000000 \times 10^{4}$
$C_1 = -6.8939127475 \times 10$
$C_2 = 3.5226118983$
$C_3 = -6.8357539823 \times 10^{-2}$
$C_4 = 1.5832717315 \times 10$
$C_5 = -2.64181230471 \times 10^{-6}$
$C_6 = 3.6093303138 \times 10^{-9}$
$C_7 = -2.5555598476 \times 10^{-12}$
$C_8 = 8.5635041641 \times 10^{-16}$
$C_9 = -1.0717599406 \times 10^{-19}$
$C_{10} = 0.2195902219$
$C_{11} = 0.06387370699$
$D_1 = 7.4165322904 \times 10$
$D_2 = -1.5834400475$
$D_3 = 3.8530771011 \times 10^{-3}$
$D_4 = 8.0133713668 \times 10^{-4}$
$D_5 = -8.9203123846 \times 10^{-7}$
$D_6 = 8.9059711315 \times 10^{-10}$
$D_7 = -5.3779372664 \times 10^{-13}$
$D_8 = 1.7398277309 \times 10^{-16}$
$D_9 = -2.3084044942 \times 10^{-20}$
$E_1 = 2.3083514362 \times 10^{-1}$
$E_2 = -9.3636207171 \times 10^{-1}$
$E_3 = 9.0339184652$
$E_4 = -4.1832067163 \times 10^{2}$
$E_5 = 1.0897627893 \times 10$
$E_6 = -1.2913856376 \times 10^{2}$
$E_7 = 5.9782049913 \times 10$

where B_1 to B_9 are constants. This relation has been derived by a least squares fit to the data of Baehr et al. (Ref 8).

3.3 Thermal Conductivity

Following Ziebland (Ref 9) and Jacobsen et al. (Ref 10), the thermal conductivity, *k*, can be expressed as:

$$k = \sum_{i=1}^{9} C_i T^{(i-3)} + C_{10}\rho + C_{11}(e^{3.6\rho} - 1.0) + \frac{\beta\sigma T^2}{C_{12}}\left(\frac{\partial P}{\partial T}\right)_\rho \quad \text{(Eq 3)}$$

where σ is the Boltzmann's constant, β is the coefficient of thermal expansion, and C_1 to C_{12} are empirical constants. The first term on the right of Eq 3 is the dilute gas contribution, the second term is the excess or dense fluid contribution, and the third term is the enhancement due to the influence of the critical point (Ref 10).

3.4 Coefficient of Thermal Expansion

Equation 1 can be used to determine the coefficient of thermal expansion β from the following definition:

$$\beta = \frac{1}{V}\left(\frac{\partial V}{\partial T}\right)_P \equiv \frac{1}{\rho}\frac{1(\partial P/\partial T)_\rho}{\rho(\partial P/\partial \rho)_T} \quad \text{(Eq 4)}$$

3.5 Viscosity

The viscosity of nitrogen can be calculated from the expression (Ref 10):

$$\mu = \sum_{i=1}^{9} D_i T^{(i-3)} + \sum_{j=1}^{7} E_j \rho^j \quad \text{(Eq 5)}$$

where D_i and E_j are constants. The first term on the right hand is the dilute gas contribution, and the second term represents the excess or dense fluid contribution (Ref 10).

The heat capacity, viscosity, and thermal conductivity obtained from Eq 1 to 5 are used to define the Prandtl number *Pr*:

$$Pr = \frac{C_p \mu}{k} \quad \text{(Eq 6)}$$

The values of the constants appearing in Eq 1 to 5 are summarized in Table 1. The operating conditions used for the casting process simulated (Fig. 2) are presented in Table 2.

Table 2 Operating parameters used in the study

Temperature of molten Al alloy, K	993
Preheat temperature of preform, K	923
Operating pressure, MPa	5.52
Ambient temperature, K	298
Height of mold, m	0.388

4. Determining the Heat Transfer Coefficient at High Pressure

The heat transfer coefficient *h* at high pressure depends on the temperature and the thermophysical properties of the ambient nitrogen in the pressure vessel, and the external surface temperature of the mold. Assuming free convective heat transfer, the Grashof number Gr_L over a length *L* is defined as:

$$Gr_L = \frac{g\beta(T_w - T_\infty)L^3}{\nu^2} \quad \text{(Eq 7)}$$

where T_w and T_∞ are respectively the mold surface temperature and ambient nitrogen temperature, *L* is the height of the mold, ν is the kinematic viscosity, and *g* is the acceleration due to gravity. For the mold with a cross section 202 mm by 202 mm and height 388 mm used in this study, the variation of the Grashof number with nitrogen temperature is plotted in Fig. 3. At the operating pressure of 5.52 MPa (800 psi) considered, Fig. 3 shows that the convection is indeed turbulent, because

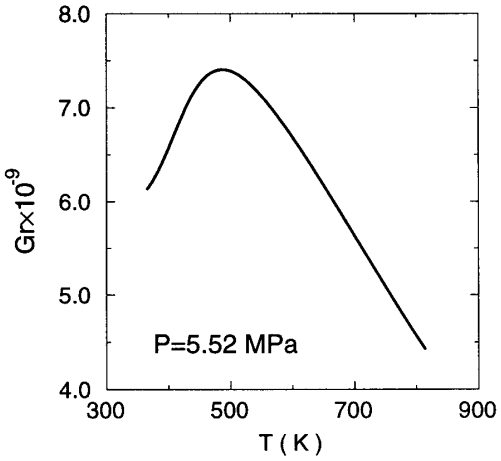

Fig. 3 Variation of Grashof number with side wall temperature

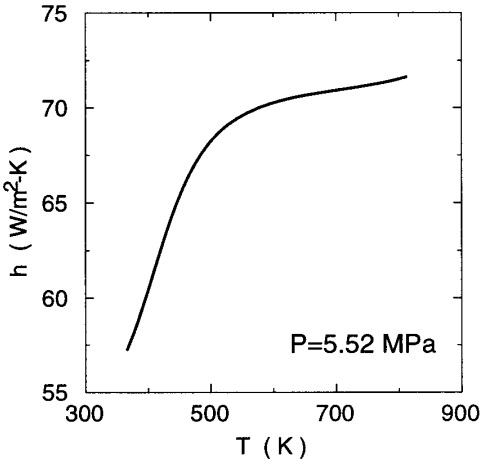

Fig. 4 Variation of average heat transfer coefficient with side wall temperature

$Gr > 10^9$ (Ref 11). Thus, the following expression is used to calculate the average Nusselt number Nu, in the turbulent regime (Ref 5):

$$Nu = 0.12(Gr_L)^{1/3}Pr^{1/3} \quad \text{(Eq 8)}$$

The average heat transfer coefficient h can thus be obtained from the expression:

$$h = \frac{Nuk}{L} \quad \text{(Eq 9)}$$

Figures 4 and 5 show the variation of h with mold surface temperature and the mean nitrogen temperature at 5.52 MPa (800 psi). Figure 6 shows the variation of h with pressure. The corresponding effect of mold surface temperature on h is presented in Fig. 7. In this turbulent regime, there appears to be a linear dependence of heat transfer coefficient on pressure at a fixed nitrogen temperature in the thermal boundary layer. On the other hand, the relationship between the heat transfer coefficient and temperature is highly nonlinear.

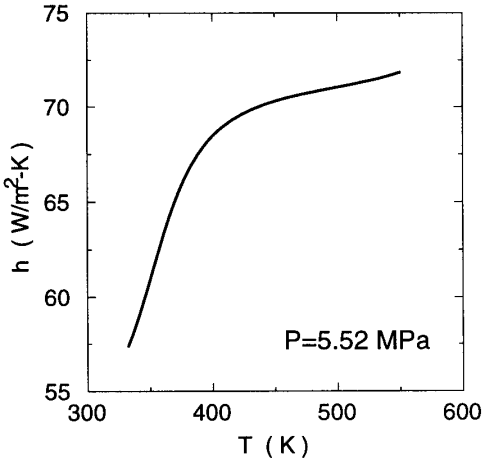

Fig. 5 Variation of average heat transfer coefficient with mean nitrogen temperature in thermal boundary layer

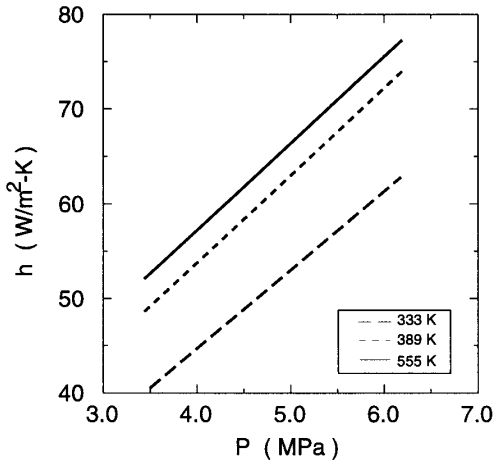

Fig. 6 Variation of heat transfer coefficient with pressure

Using multiple regression analysis (Ref 12, 13), the following approximate relationship has been established between h, P, and T for the casting operation conditions in Table 2:

$$h = -265.64 + 8.992 \times 10^{-6}P + 1.887T - 4.112 \times 10^{-3}T^2 + 2.995 \times 10^{-6}T^3 \quad \text{(Eq 10)}$$

where h is the heat transfer coefficient in W/m$^2 \cdot$ K, T is temperature in K, and P is the pressure in Pascal. This expression can be considered valid for the ambient nitrogen temperature of 298 K, the average nitrogen temperature in the turbulent thermal boundary layer in the range 333 to 555 K and the operating pressure in the range 3.45 to 6.20 MPa (500 to 900 psi).

5. Application to High Pressure Metal-Matrix Composite Casting

The high-pressure infiltration casting process typically utilizes pressurized gas (usually nitrogen) to force liquid metal into a preform of reinforcement materials. The specific casting system considered here is illustrated in Fig. 2. A bank of thermocouples placed at several locations in the mold was used to measure the temperature history during the casting process. Alumina preform was infiltrated with Al 2014 alloy at a pressure of 5.52 MPa (800 psi) and the casting was initiated shortly after. The heat transfer coefficient obtained from Eq 10 was used to express the thermal boundary condition on the lower part of the mold surface that is exposed to the ambient nitrogen in a numerical study of the solidification phenomena.

The mathematical modeling involves solution of the following equations governing the conservation of thermal energy:

$$\rho C_p \frac{\partial T}{\partial t} = \nabla \cdot (k\nabla T) + \rho L \frac{\partial f_s}{\partial t} \quad \text{(Eq 11)}$$

where T is the temperature of the composite material, ρ is the density, C_p is the specific heat, k is the heat conductivity, L is the latent heat released at the solidification front, and f_s is the solid

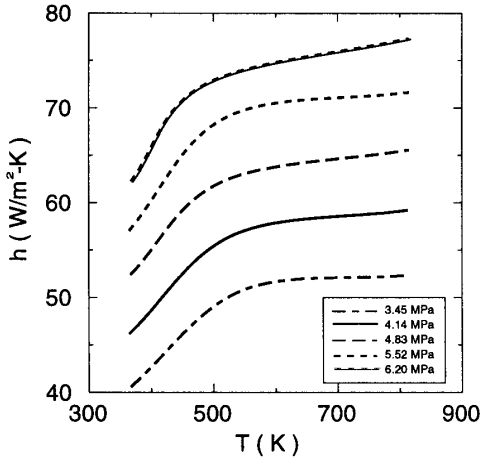

Fig. 7 Variation of heat transfer coefficient with surface temperature

fraction. Allowance is made for anisotropy of C_p, ρ, and k through the rule of mixture between the reinforcement and matrix.

The heat flux at the external surface of the mold is:

$$q = h(T_w - T_\infty) \quad \text{(Eq 12)}$$

where h is the heat transfer coefficient obtained from Eq 10, T_w is the temperature of the mold surface, and T_∞ is the ambient temperature. The bottom surface is allowed to lose heat to the chill according to the available experimental data (Ref 14).

Figure 8(a-c) show the predicted and measured cooling curves at three monitored locations identified as TC1, TC2, and TC3 in Fig. 2 in the casting mold. As expected, both sets of results demonstrate the highest cooling rates near the bottom chill. The good agreement between the measurements and the predictions validates the relation established in Eq 10.

To demonstrate the effect of pressure on the heat transfer coefficient and its consequence on the solidification pattern, the calculations at 5.52 MPa were repeated with a constant value of 55 W/m^2 · K, an approximate value to the estimated heat transfer coefficient at 3.45 MPa (Fig. 7). Figure 9 shows the predicted solidification patterns with h obtained from Eq 10 and h = 55 W/m^2 · K. Clearly, the two patterns exhibit quite remarkable differences. Specifically, the fixed value of h underestimates the cooling effect and the solidification progresses rather slowly. The use of the relationship in Eq 10, on the other hand, allows for the increase in heat transfer coefficient at the mold

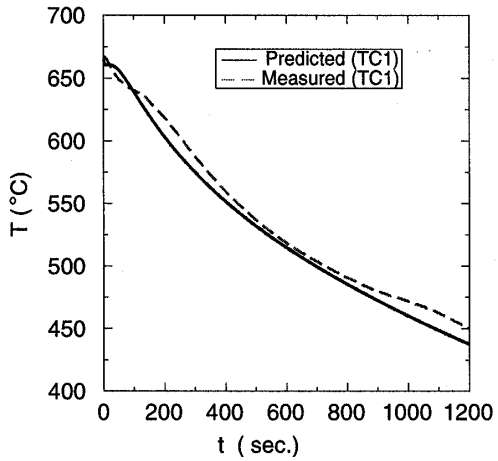

(a)

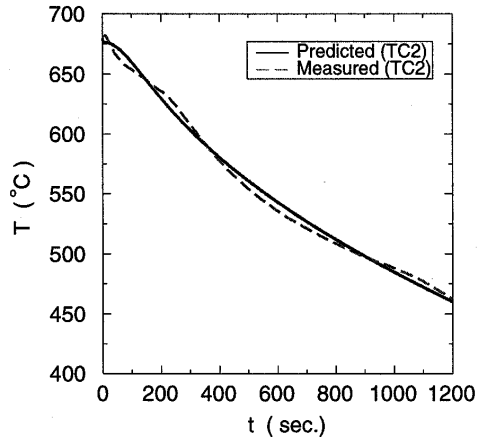

(b)

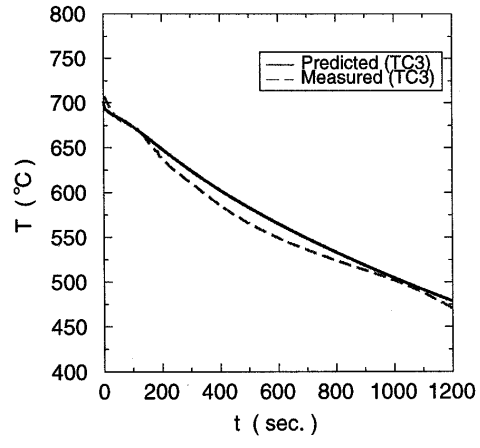

(c)

Fig. 8 Cooling curve. (a) Thermocouple location TC1. (b) Thermocouple location TC2. (c) Thermocouple location TC3

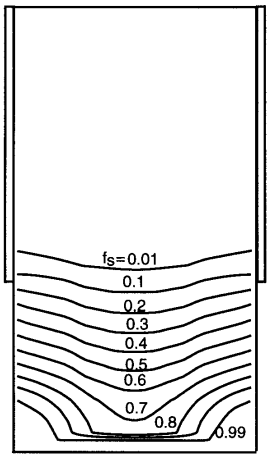

(a)

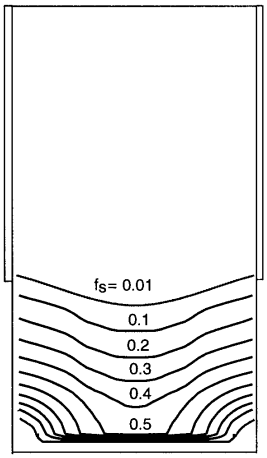

(b)

Fig. 9 Solid fraction profiles at 300 s. (a) h obtained from Eq 10. (b) h = 55 W/m^2 · K

surface with pressure, thus predicting higher cooling and solidification rates. These results suggest the need to allow for the influence of pressure on the heat transfer coefficient in processes involving high pressures, such as the casting of certain metal-matrix composites.

6. Conclusions

A correlation has been established between the heat transfer coefficient on the external surface of a mold and the temperature and pressure of the ambient gas (nitrogen), within the operating range typical of pressure-infiltration casting of metal-matrix composites. This correlation is based on existing data and relationships between the thermophysical properties of the ambient gas and its pressure and temperature. The predicted temperature profiles based on this correlation are in good agreement with the experimental data obtained in a pressure-infiltration casting system. The results also show significant influence on the solidification pattern of application of appropriate heat transfer coefficient at the operating pressure. Similar heat transfer correlations can be readily determined for other casting systems once the geometry and operating conditions are fully specified.

Acknowledgments

The project was supported by grants from Metal Matrix Cast Composites, Inc. and the National Science Foundation under contract No. DMI-9619198, Delcie Durham, Program Director. The authors are grateful for the useful discussion with Dr. J.A. Cornie and Dr. R. Mason, who also provided the experimental data.

References

1. A.J. Ede, Advances in Free Convection, *Advances in Heat Transfer,* J.P. Hartnett and T.F. Irvine, Jr., Ed., Vol 4, Academic Press, 1967, p 1-64
2. S.W. Churchill and R. Usagi, A General Expression for the Correlation of Rates of Transfer and Other Phenomena, *A I Ch E J.*, Vol 18, 1972, p 1121-1128
3. S.W. Churchill and H.H.S. Chu, Correlation Equations for Laminar and Turbulent Free Convection from a Vertical Plate, *Int. J. Heat Mass Transfer,* Vol 18, 1975, p 1323-1328
4. R.L.C. Bosworth, *Heat Transfer Phenomena,* John Wiley & Sons, 1972, p 101
5. O.A. Saunders, Effect of Pressure upon Natural Convection in Air, *Proc. R. Soc. A,* Vol 157, 1936, p 278-291
6. F.J. Bayley, An Analysis of Turbulent Free Convection Heat Transfer, *Proc. Inst. Mech. Eng.*, Vol 20 (No. 169), 1955, p 361-370
7. R.T. Jacobsen, R.B. Stewart, and A.F. Myers, An Equation of State for Oxygen and Nitrogen, *Advances in Cryogenic Engineering,* Vol 18, 1973, p 248-255
8. H.D. Baehr, H. Hartmann, H.C. Pohl, and H. Schomacker, *Thermodynamische Funktionen Idealer Gase fuer Temperaturen bis 6000 K* (in German), Springer-Verlag, Berlin, 1968
9. H. Ziebland and J.T.A. Burton, The Thermal Conductivity of Nitrogen and Argon in the Liquid and Gaseous States, *Brit. J. Appl. Phys.*, Vol 9, 1958, p 52-59
10. R.T. Jacobson, R.B. Stewart, R.D. McCarty, and H.J.M. Hanley, Thermophysical Properties of Nitrogen from the Fusion Line to 3500 R (1944 K) for Pressures to 150,000 PSIA, *NBS Note 648,* 1972
11. S. Kakaç and Y. Yener, *Convective Heat Transfer,* 2nd ed., CRC Press, Inc., 1994, p 311-373
12. P. Janzow et al., *The Student Edition of MATLAB,* Prentice Hall, 1992
13. R.L. Scheaffer and J.T. McClave, *Probability and Statistics for Engineers,* 2nd ed., Duxbury Press, 1986, p 390-438
14. J.A. Cornie, *Private Communication,* 1997